International Journal of Fluid Power 14 (2013) No. 1 pp. 47-56

DESIGN, FABRICATION, AND EVALUATION OF A DISTRIBUTED PISTON STRAIN-ENERGY ACCUMULATOR

John M. Tucker and Eric J. Barth

Laboratory for the Design and Control of Energetic Systems
Department of Mechanical Engineering – Vanderbilt University, Nashville, Tennessee
eric.j.barth@vanderbilt.edu

Abstract

By utilizing multiple energy domains, hybrid vehicles seek to harness the strengths of each domain in order to make up for the weaknesses of the other. Hydraulic hybrids in particular offer a solution to regenerative braking that exploits the power density, transmission flexibility, and rugged efficiency that hydraulic technology offers. Hydraulic regeneration utilizing an accumulator is not hampered by the relatively low power density of electric batteries, and offers greater opportunity for safer, more distributed storage than strictly mechanical regeneration techniques. This paper presents the design and experimental results-based projected performance of a distributed piston strain energy accumulator. By storing energy as strain energy in a material, strain energy accumulators offer the potential of increased energy density, efficiency and lower maintenance over gas-charged accumulators. Material selection for a strain energy accumulator is discussed for polyurethane materials with regard to hyperelastic behavior, Mullins effect and hysteresis. Experimental testing of polyurethane bladders and uniaxial tension specimens is presented, with the highest performers showing 15 kJ/l with 17 % loss hysteresis. Design tradeoffs for different configurations of a strain energy accumulator is presented, with a detailed analysis of a distributed piston elastomeric accumulator (DPEA). A prototype DPEA accumulator was constructed and experimentally evaluated with two different polyurethane materials. These experimental results are then utilized to project a full scale device with regard to its overall system energy density. These projections are compared to an idealized gas-charged accumulator.

Keywords: Strain-energy storage, hydraulic accumulator, elastomerics

1 Introduction

In recent years, increased attention has been given to hydraulic gas charged accumulators for their potential as high power-density energy storage devices, particularly in the case of hydraulic hybrid vehicles. A hydraulic hybrid equipped with regenerative braking can utilize its hydraulic drive to capture the vehicle's kinetic energy and store it in an accumulator rather than discharging it as heat like dissipative brakes. This energy can then be returned back to the vehicle through the same pump/motor(s) used to slow it down. The high power-density of hydraulic pump/motors allows them to store and return this energy much more quickly than electric hybrids. Since braking of a vehicle happens over only a handful of seconds, any energy that the hybrid drive cannot absorb in that time must be dissipated and is therefore lost. Since the charging power density of a battery is proportional not only to the energy density, but also to the inverse charging time, even high end Li-ion batteries have inadequate charging power densities for hydraulic hybrid applications. With recommended minimum charge times between 1 and 2 hours (Thapa, 2007), their high energy density of 700 kJ/kg translates to a mere 0.15 kW/kg of power density. Ultimately, this means that while a 0.3 kg battery is capable of storing the kinetic energy of a small urban vehicle traveling at 50 km/hr (about 30 mph), a 275 kg battery is required in order to absorb that energy in a 5 second braking window. Because of this disparity in power density, hydraulic hybrids have a much greater potential for fuel savings through regenerative braking in small urban vehicles.

One current limiting factor for hydraulic regenerative braking is the energy density and efficiency of the accumulator. While batteries are limited by how quickly they can be charged, they can store large amounts of energy for long periods of time without losing their

This manuscript was received on 09 August 2012 and was accepted after revision for publication on 21 November 2012

charge. Hydraulic gas charged accumulators, by contrast, have relatively low system energy densities in the neighborhood of 8 kJ/L (Li, et al. 2007) and can leak thermal energy to their environment over time, depending upon their design. Pourmovahed et al. (1988) showed that with as little as 50 seconds passing between gas compression and expansion, a piston-type gas accumulator's efficiency can fall to about 60 %. Despite promising solutions to this thermal inefficiency, such as the insertion of elastomeric foam as a regenerator (Pourmovahed, 1988), gas accumulators have a fundamental maintenance cost associated with pressurized gas diffusing into the hydraulic working fluid. In order to address these and other issues with conventional gas accumulators, this paper proposes a switch from compressed gas to material strain as an energy storage medium. By storing energy in the strain-energy domain rather than the thermal domain (compressible gas), one can eliminate the problem of gas diffusion and can increase energy density based upon the properties of the strained material.

For applications like hydraulic hybrids, both gravimetric and volumetric system energy density are important. The gravimetric energy density of the device will depend on material selection choices for the exterior of the device (steel, carbon fiber, etc) but these design choices will be out of the scope of this paper. The primary goal and scope of this work is to elucidate the design tradeoffs regarding elastomeric material properties, the effect of dead volume, and system pressure; the optimized design of the housing and other structural components to achieve a maximum gravimetric energy density for a given volumetric energy density is largely a decoupled problem.

2 Energy Density

Two critical properties when designing a strain energy accumulator for a hybrid vehicle are energy density, and efficiency. Strain energy density of an elastic material is defined as the amount of strain energy that can be absorbed by a material before it irreversibly deforms per unit mass of the material. It can also be defined in terms of unit volume (volumetric energy density) which is related to gravimetric energy density by the specific mass of the material. In this way, a material's strain energy density can be written as a pressure since 1 kJ/L is equivalent to 1 MPa:

$$e_M = \frac{E_{Stored}}{\forall_M} = \int_{\varepsilon 1}^{\varepsilon 2} (\sigma) d\varepsilon \qquad (1)$$

This is convenient for hydraulic systems, because it allows a clear comparison between the relative role of the average operating pressure and strain energy density. Since power is the product of pressure and flow rate, energy transfer is the integral of pressure over a volumetric displacement. By using the mean value theorem, one can represent the energy transferred per unit volume of fluid simply by calculating the average fluid pressure:

$$e_f = \frac{E_{Stored}}{\forall_F} = \frac{1}{\forall_F} \int_0^{\forall_F} (P) d\forall_F = \frac{\forall_F}{\forall_F} P_{avg} = P_{avg} \qquad (2)$$

If this flow is either into (or out) of a closed vessel, this indicates the energy stored (or released) per unit volume of fluid regardless of the mechanism that produces the pressure. In our case, the mechanism will of course be the strain energy in the elastomeric material that surrounds the trapped fluid. The quantity defined by Eq. (2) will be referred to as the fluid specific energy density and denoted by e_f. It is important to note that this does not imply that the energy is stored by the fluid. In developing design metrics, it will be useful to interchange the notion of the energy stored per unit volume of the fluid, and the average pressure.

Since a hydraulic strain energy accumulator requires both working fluid to transfer energy and deformable material to store the energy, both volumes must be taken into account. The energy densities of these components can be combined with other dead volumes $\forall_D$ of the system - such as fittings, hose lines, valves, and pressure vessel walls - to form the overall system energy density where the energy stored is divided by the sum of the material volume, the fluid volume and the dead volume:

$$e_{system} = \frac{E_{Stored}}{\frac{E_{Stored}}{e_M} + \frac{E_{Stored}}{P_{avg}} + \forall_D} = \frac{1}{\frac{1}{e_M} + \frac{1}{P_{avg}} + \frac{\forall_D}{E_{Stored}}} \qquad (3)$$

Since overall system energy density is a sum of inverse sums, it is necessarily less than the smallest of its components. In practice this means that increasing average hydraulic pressure of the system will not increase the system energy density beyond the strain energy density of the material, or vice versa. However, if the fluid specific energy density and the material strain energy density are equivalent, the total system energy density will be one half of this value. Recognizing this relationship helps to determine the relative emphasis which should be placed on trying to improve on each component. At the time of this paper, the current state of hydraulic pump/motors, valves, seals, and fittings set the hydraulic pressure ceiling between 34.5 and 68.9 MPa (5000 and 10,000 psi). Being equal to the average pressure, the fluid specific energy density is therefore limited on the order of 50 MPa (or 50 kJ/L). This means that in order to be competitive with conventional gas bladder accumulators in terms of system energy density, a strain energy accumulator must have a strain energy density of at least 10 kJ/L with very little dead volume. Even higher strain energy densities are required if the actual fluid specific energy density is significantly lower than the maximum theoretical.

3 Material Selection: Optimizing e_M

Because strain energy density is the integral under the stress-strain curve, a material which excels in strength may have a much smaller energy density than a weaker material that is capable of higher elongations. Spring steel, for example, has a maximum stress of about 500 MPa with a Young's modulus of 210 GPa. This gives a calculated maximum strain of 2400 microstrain, or 0.24 % elongation. Assuming linear elasticity, the integral of this stress strain curve can be

estimated. For spring steel, $e_M \cong 0.6$ MPa = 0.6 kJ/L, less than 10 % of the strain energy density required for this application. Polyurethanes, on the other hand, while having maximum stresses on the order of 40 MPa or less, are capable of strains up to 600 %. As shown in Pedchenko and Barth (2009) the product of yield stress and elongation for polyurethane is among the highest of all materials. The assumption of linear elasticity is invalid for polyurethanes, because they are hyperelastic by nature. Even so, as will be demonstrated in this paper, our measurements show a strain energy density of 15 MPa for a particular material tested, twenty five times that of spring steel and above the minimum requirements of this application. Given that this material was not specifically engineered for a high strain energy density, this measured value should be taken as a lower bound to the potential that elastomeric materials hold. Indeed, material selection software indicates volumetric and gravimetric strain energy densities as high as 100 kJ/L and 100 kJ/kg (CES Selector ver. 4.8.0. Granta Design Limited. Build 2008, 2, 29, 1).

In addition to strain energy density, however, mechanical efficiency is paramount for a strain energy accumulator to be effective. The percentage of mechanical energy returned by a material once it is strained varies tremendously from material to material. As seen in Fig. 3, even among polyurethanes, this efficiency can range from as low as 60 % to well above 80 %. In this paper, a particular formulation of thermoset polyurethane is investigated in terms of its strain energy density and efficiency as well as its optimum peak stress.

3.1 A Brief Background on Polyurethane

The name polyurethane applies to a wide array of polymers ranging from soft upholstery foam to hard shopping cart wheels. Many formulations of polyurethane are rubberlike elastomers with exceptionally high yield strains. Among these are thermoset polyurethanes, which typically have high elasticity and resistance to abrasion. These polyurethanes can range in tensile strength from less than 6.9 MPa (1000 psi) to more than 48 MPa (7000 psi). Their maximum elongation before break can similarly range from less than 100 % to more than 600 %. As stated above, polyurethanes are hyperelastic materials. Their modulus of elasticity decreases as a function of strain up to a point, beyond which it increases. This nonlinearity makes precise prediction of strain energy density difficult from manufacturer reports alone. Often these reports list the stress needed to achieve 100 % elongation, 300 % elongation, or both. These points, however, provide little insight into the overall stress-strain profile. In addition to the nonlinearity of the stress-strain profile, a softening phenomenon called the Mullins effect occurs as polyurethanes are strained. When these materials are strained for the first time after a certain recovery period, they follow an initial stress-strain curve for loading and unloading. On subsequent cycles, however, the material behaves in a softer manner until it reaches the previous maximum strain. Each time the material is strained to a new maximum, the subsequent behavior is modified. Figure 1, taken from Diani's investigation (Diani, et al.

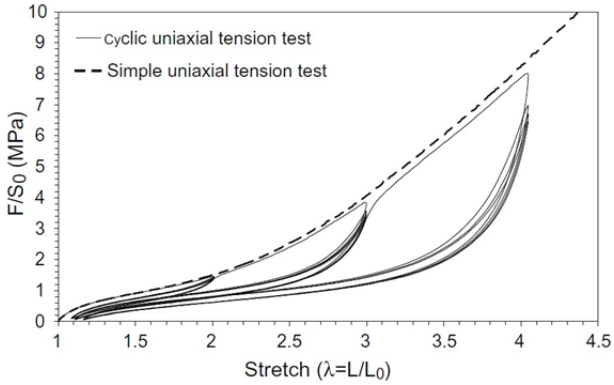

Fig. 1: *Stress-strain responses of a 50 phr carbon-black filled SBR submitted to a simple uniaxial tension and to a cyclic uniaxial tension with inceasing maximum stretch every 5 cycles (Figure taken from Diani, et al., 2009).*

2009) on the Mullins effect clearly demonstrates this effect as two identical samples are stressed, one strained cyclically in three stages, and the other strained to the maximum only once.

It is easy to see from Fig. 1 how the 100 % modulus as recorded from a single tension test will not be equal to the stress seen at 100 % elongation once 300 % elongation has been previously applied. Furthermore, the hysteresis - the efficiency of strain energy return - is very different after the first cycle. Because neither strain energy density nor efficiency can be extrapolated from a single tensile test or recorded property, the stress-strain behavior must be observed from cyclical experimentation.

3.2 Material Selection

The particular formulation of thermoset polyurethane was selected from a range of polyurethanes by use of a material selection apparatus. This apparatus shown in Fig. 2 allowed diaphragms of various elastomers to be mounted and inflated pneumatically from one side into a water-filled expansion chamber. Displacement of the water could then be measured along with the inflation pressure behind the diaphragm. The integral of this pressure-volume behavior corresponds to the energy stored in the diaphragm during inflation. When the gas was vented slowly from behind the diaphragm, the integral under the discharging pressure-volume curve equates to the energy returned during deflation.

This apparatus allowed for the rapid comparison of a wide selection of polyurethanes both in terms of energy stored and percent energy return. Figure 3 shows the pressure-volume curves of 13 different diaphragms. The legend lists the Shore durometer and thickness of each diaphragm as well as the % energy lost for each formulation. The black, 90A Shore durometer polyurethane from Pleiger Plastics Company showed the best performance from the materials tested, storing about 4 kJ per liter material and returning 84 % of the stored energy.

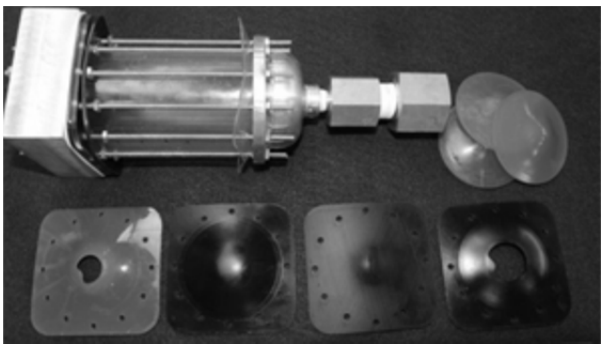

Fig. 2: *Diaphragm test apparatus and post-test diaphragms*

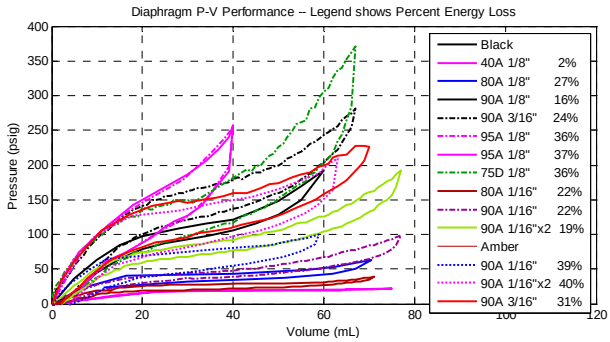

Fig. 3: *Comparison graph of various polyurethane diaphrams. Areas beneth charging curves represent energy storage. Areas beneth discharging curves represent energy return. Areas within hysteresis loops represent energy losses, which are also recorded in the legend*

The test apparatus was not designed to find the actual energy storage limits of each material, but rather to compare their relative performance. Each of these materials have reported maximum elongations of 500 % to 600 %, while an inflated diaphragm experiences between 100 % and 130 % average elongation and a broad strain gradient within the material. The tests therefore show cyclical results for a broad range of repeated peak strains within each material. This type of test is somewhat analogous to testing the closed-loop response of a control loop by subjecting it to a step reference command that contains many frequency components.

By increasing the total stress placed on the material by loading it uniformly, more energy can be stored and the demonstrated energy density increases. However, if stress exceeds a certain limit, the material properties begin to degrade after very few cycles. Batteries of tensile tests were therefore performed on the selected polyurethane in order to determine the optimal peak stress. Four sections of the polyurethane were lasercut into dog bone tensile specimens and cyclically loaded to their assigned peak stresses. The first through fourth specimens were loaded to a maximum stress of 14.48 MPa (2100 psi), 16.55 MPa (2400 psi), 17.24 MPa (2500 psi), and 19.65 MPa (2850 psi), respectively. Figure 4 shows the stress-strain curves of the third sample. The legend shows the % energy lost in each cycle followed by the measured energy density in J/L.

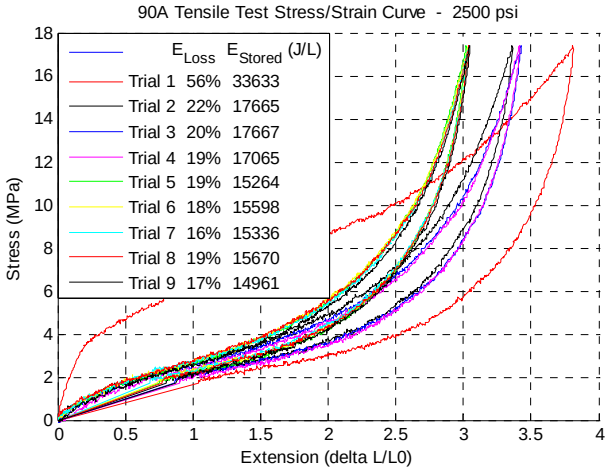

Fig. 4: *uniaxial tensile test results for polyurethane 90A, sample 3. Maximum stress set to 17.2 MPa (2500 psi)*

Table 1 summarizes these results for all four specimens. As expected, the energy density increased with increasing peak stress up until some optimum value.

Table 1: Tensile Test Results

σmax (MPa)	14.48	16.55	17.24	19.65
(psi)	2100	2400	2500	2850
eM (kJ/L)	13.8	14.4	15.4	13.4
ELoss (%)	20.0	20.8	17.8	21.8
St. Dev. (%)	0.8	0.8	1.3	4.7

These results demonstrate the aforementioned potential for thermoset polyurethanes in terms of strain energy density. Furthermore, they underline a necessary step in the design of strain-energy accumulators. When determining the maximum load to which an accumulator should be charged, cyclical tensile testing must be performed on the chosen elastomer, because the optimal stress can be as little as one half the reported tensile strength of the material: 17.24 MPa (2500 psi) compared to 38 MPa (5500 psi) in the case of this polyurethane. Lastly, it should be underscored that this selection represents a lower bound given that these particular material formulations were not specifically engineered to exhibit high energy density and low hysteresis.

4 Design Metrics

Three central design metrics were considered for developing or evaluating a strain energy accumulator for a hydraulic hybrid vehicle: pressure-volume curve shaping, maximizing material utilization, and minimizing dead volume. These relate directly to the three components of Eq. 3.

4.1 Pressure-Volume Curve Shaping: Raising P_{avg}

Recall that energy is transferred to a hydraulic accumulator as the time integral of pressure times volumetric flow rate. Equation 2 shows that the average

pressure of an accumulator determines its fluid specific energy density and therefore required fluid volume, with a higher average pressure corresponding to a lower volume requirement. Maximum system pressure is - barring other limitations - fixed by the pressure ratings of the hydraulic pumps, valves, fittings, and lines. Therefore, in order to maximize average pressure - so that fluid volume is minimized - the pressure throughout charging should be as close to the maximum pressure as possible. An ideal hydraulic accumulator would have a constant pressure and a correspondingly flat pressure-volume curve.

Hydraulic strain energy accumulators obtain their pressure-volume curves by having fluid act, directly or indirectly, upon a deformable material. The stress-strain curve of the deforming material is translated into a pressure-volume curve through some transmission ratio, dependent upon the design of the accumulator. Just as a crankshaft changes its force-to-torque ratio as a function of crank angle, the stress-to-pressure ratio of a hydraulic accumulator need not be constant. In any given configuration, the fluid has some mechanical advantage (or disadvantage) which translates material stress into fluid pressure. If this ratio were held constant, the pressure-volume curve of the accumulator would have the same shape as the stress-strain curve of the material. In the case of a Hookean material, this shape would be a line of constant slope, with an average value equal to one half the maximum value. In the case of hyperelastic materials like polyurethane, this shape looks even less like the ideal pressure-volume curve and has an average value closer to one third of its maximum (Fig. 4).

In order to rectify this situation, the concept of variable mechanical advantage can be leveraged. If the ratio of fluid pressure to material stress can be lowered from a value much greater than 1:1 to a value much closer to 1:1 as the accumulator fills, the average fluid pressure can be raised towards the maximum pressure value. Given equal maximum pressure values and equal energy storage capacities, a design which incorporates this feature will require less fluid volume to charge than a design with constant mechanical advantage. It should be noted that this assumption of equal maximum pressure values only holds true if sufficiently stiff materials exist. A falling ratio of fluid pressure to material stress (increasing mechanical advantage with fill volume) cannot be paired with a high maximum system pressure if the combination dictates a material strength beyond the range of materials available.

One example of variable mechanical advantage is a thin-walled cylindrical balloon (Pedchenko and Barth, 2009). When inflated, it seems to behave at first like a linear system, with pressure rising sharply in proportion to volume. However, at a certain pressure a bubble begins to form which rapidly expands to some maximum diameter. A plot of the pressure-volume curve of such an inflation reveals that the pressure actually drops somewhat during the formation of this bubble. The reason for this phenomenon is twofold. First, the material is hyperelastic, which means that its modulus of elasticity decreases significantly at moderate levels of strain before increasing at higher levels of strain. Second, as the bubble begins to form, the cross-sectional area of fluid (or air) acting on the bubble is increasing. This means that the axial load acting on the material cross-section is much greater along the bubble than along the rest of the balloon. The fluid has a local mechanical advantage at the bubble greater than it had before bubble formation (Fig. 5).

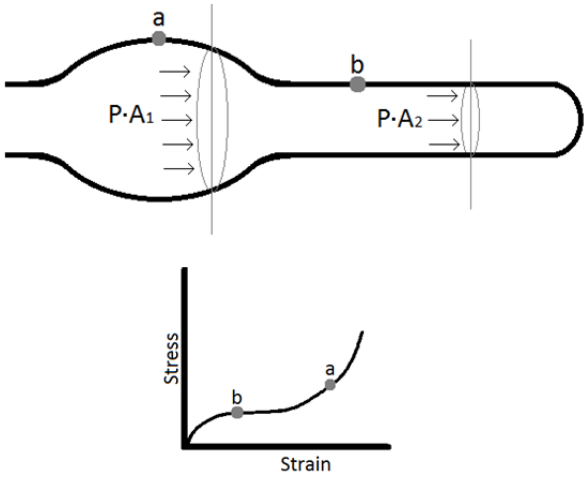

Fig. 5: *Bubble propagation phenomenon. Pneumatic pressure acts along larger cross-sectional area at bubble. Bubble exists between 'a' and 'b' on the stress-strain curve.*

The hyperelastic and mechanical advantage effects combine and result in the unstable bubble formation, which only halts once the modulus of elasticity has increased sufficiently (assuming a continuous source of fluid). The balloon can now be thought of in terms of three distinct regions. First, there is an underinflated region where the material still behaves elastically. Second, there is the apex of the bubble where the modulus of elasticity has climbed sufficiently; this region no longer expands radially. Third, there is the taper of the bubble which bridges the first two regions on both sides of the bubble. This is the region where strain continues to occur at a constant pressure. This region does not change in size, but rather it propagates down the length of the balloon, effectively converting more and more of the first region into more and more of the second region. This example is a rather unique case where the mechanical advantage of the fluid on the material varies not with time but with position along the material. The end result is a nearly flat pressure-volume curve, baring the spike of pressure that occurs when the bubble first forms. As discussed above, this low ratio of fluid pressure to material stress limits the maximum system pressure based on wall thickness and material strength.

4.2 Maximizing Material Utilization: Achieving e_M

While pressure-volume curve shaping can help to raise fluid specific energy density, overall system energy density is still limited by the effective strain energy density. The strain energy density of the candidate polyurethane has been demonstrated to exceed 15 kJ/L, but this value is taken from a uniaxial tensile test. In uniaxial tension, all of the specimen's gage length was

equally strained, maximizing the energy storage for a fixed peak stress. In general, however, the material in an accumulator may not be strained equally throughout, leading to a lower average energy density of the material. A prime example of this phenomenon is a thick-walled bladder. When inflated, the inner wall of the bladder experiences much higher stress and strain than the outer wall and will therefore reach peak stress long before the rest of the bladder. Consequentially, more elastomer is required to store a fixed amount of energy. In order to minimize the volume of required elastomer, a strain energy accumulator must therefore maximize its material utilization by uniformly straining the material when fully charged.

An elastomeric balloon-type accumulator with relatively thin walls (where the wall is of small thickness compared to the vessel diameter) achieves a more uniform strain of the material and can more fully achieve the maximum strain energy density allowed by the material. However, the limitation of this extreme is a lower system pressure, which by definition, leads to a lower fluid specific energy density. A strain energy accumulator design is therefore needed that does not adversely lower the system pressure in addition to straining the material uniformly.

4.3 Dead Volume: Minimizing $\forall_D$

Sections 4.1 and 4.2 give guidelines for maximizing hydraulic and strain energy density. However, as seen in Eq. 3, one last contribution exists which can lower the overall system energy density. The dead volume $\forall_D$ is the volume of the accumulator that does not contribute directly to the energy transfer or storage. Minimizing this volume is essential, and yet this task can sometimes come in direct conflict with the other design metrics. Consider again the example of a simple elastomeric bladder. A thin-walled bladder provides beneficial curve shaping and material utilization. However, compared to a thick-walled bladder, it has a much larger volume of fluid than volume of wall material, even at zero strain. This initial volume of fluid does not contribute to energy transfer or storage and is therefore dead volume. Using a thin wall rule of thumb, where the diameter is at least ten times as large as the thickness, the dead volume of fluid is consequently at least 77 % larger than the volume of wall material. Initial fluid within the bladder is not the only contributor to dead volume. Elastomers in tension require specialized grips to hold them. Both the section of material being gripped and the grips themselves contribute to dead volume. Great care must be taken to balance the role that dead volume plays along with the other two design metrics in order to ensure the maximum overall system energy density.

5 Distributed Piston Elastomeric Accumulator

The problem of minimizing dead volume while maximizing material utilization and achieving an adequate system pressure is intractable in the case of a simple bladder inflated from within. In order to reap some of the potential benefits of the bladder's variable mechanical advantage, however, a design was developed based upon the idea of turning a bladder inside out. The Distributed Piston Elastomeric Accumulator (DPEA) in its simplest form consists of a rodless hydraulic piston-cylinder device with its piston tethered to one cylinder end by an elastomeric cord.

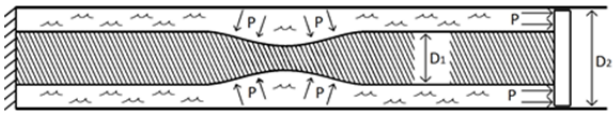

Fig. 6: *DPEA schematic. Hydraulic pressure acts upon initial piston annulus and along length of elastomer card*

As fluid is pumped into the cylinder alongside the cord, the piston is forced to move in a way which stretches the cord. As the cord thins, the fluid cross-sectional area grows, increasing the mechanical advantage of the fluid on the device. Some of the driving force is distributed along the length of the elastomeric cord as it tapers from its thickest region at the piston to its thinnest point. For this reason the term "distributed piston" is used. In this way, the DPEA retains some of the pressure-volume curve shaping that a simple bladder has. By setting the initial ratio of material volume to fluid volume $\forall_m/\forall_{f0}$ very high, the dead volume is minimized like in the case of a very thick-walled bladder. However, unlike a thick-walled bladder, the DPEA uniformly distributes strain throughout its cross-section; the interior does not experience more or less strain than the exterior. It is unclear whether or not a sufficiently high ratio of initial material volume to fluid volume will result in the constant pressure bubble propagation seen in cylindrical balloons, because the highest area ratio of the successfully assembled prototypes was 6.1:1 with a non-constant pressure profile. However, the higher the initial ratio of material volume to fluid volume is set, the greater the swing in mechanical advantage will be.

While the notion of variable mechanical advantage is qualitatively satisfying, the well-defined piston position of the DPEA provides more quantitative insight into the relationship between strain energy density and fluid specific energy density. Because solid elastomers are incompressible (their volumes do not significantly change as a function of pressure), the position of this rigid piston is directly proportional to the amount of fluid that is pumped into the accumulator. Because the elastomeric cord is in tension and is radially symmetric, its strain is also directly proportional to piston position. Therefore, for a given peak strain, the amount of fluid required to generate this strain can be calculated. This knowledge allows one to calculate the ratio between fluid specific energy density and strain energy density as a function of the peak strain and initial volumetric ratio. Consider for example a cord stressed to a peak strain of 300 % with a 1:1 ratio of material volume $\forall_m$ to initial fluid volume surrounding the cord $\forall_{f0}$. The initial volume in the high pressure side of the accumulator is therefore $\forall_{f0} + \forall_m = 2\forall_m$. When the accumula-

tor is charged, the piston in this case would traverse a distance equal to 300 % of the original cord length. The final volume is therefore four times the initial volume: $4(\forall_{f0} + \forall_m) = 8\forall_m$. Equivalently, the final volume can be written as the initial volume plus the added fluid volume: $2\forall_m + \forall_f$. Equating these two expressions for the final volume yields: $\forall_f = 6\forall_m$. The volume of working fluid required - not counting the initial dead volume of fluid $\forall_{f0}$ - is six times as large as the elastomer volume. The fluid specific energy density is therefore 16.7 % of the strain energy density.

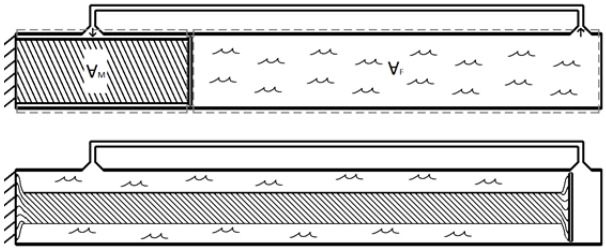

Fig. 7: *Schematic representation of DPEA volume requirement based on conservation of volume in incompressible systems*

Consider instead a much stiffer cord which stretches to a maximum elongation of 85 % and has an initial ratio of 9:1. Here the fluid specific energy density comes out to be 106 % of the strain energy density. Although softer materials can have higher strain energy densities than stiffer ones - as demonstrated by the comparison of polyurethane to spring steel - this accumulator type gives clear preference to stiffer materials in terms of fluid specific energy density e_f. The formula for this ratio in terms of peak strain ε_{max} and initial volume ratio $\forall_m/\forall_{f0}$ is:

$$\frac{e_f}{e_M} = \frac{1}{\varepsilon_{max}*\left(1+\frac{\forall_{f0}}{\forall_m}\right)} \quad (4)$$

It is important to note that this relationship does not apply to all accumulators in general but rather results from the rigid piston of the DPEA which defines a control volume of constant area which lengthens in proportion with the elastomer. Still, the equation is useful for evaluating overall system energy density for candidate materials in the context of a specific, well defined accumulator design. Equation (4) is derived from simple geometric considerations of the initial and final states of the DPEA accumulator as illustrated in Fig. 7. These considerations take into account the DPEA fluid volume, material volume, and dead space as they relate to the strain: $\varepsilon = (L_f - L_0)\ A\ /\ L_0A = \forall_f\ /\ /\forall_{M\ +\ }\forall_{f0})$, and the fact that $e_f = E_{stored}\ /\ \forall_f$ and $e_M = E_{stored}\ /\ \forall_M$

6 DPEA Prototype

In order to validate the DPEA as an effective means of leveraging variable mechanical advantage, a low pressure prototype was constructed using a softer formulation of polyurethane of Shore durometer 40A. 40A polyurethane yields a lower pressure and required gripping force than the harder 90 A polyurethane while possessing similar hyperelasticity. A hollow tube of the polyurethane, with an outer diameter of 1" (2.54 cm) and an inner diameter of 0.375" (0.9525 cm) was anchored to the piston of a 1" (2.54 cm) bore piston-cylinder device. Fluid was pumped via electric pump-motor into the cylinder until the piston traveled 200% of the unstretched gage length of the specimen. This process was cycled multiple times to exhaust the acyclical Mullins effect.

Fig. 8: *Hydraulic piston-cylinder setup*

Uniaxial tensile testing was also performed on this new polyurethane in order to calculate the varying relationship between tensile stress and working fluid pressure.

The tensile stress data measured as shown in Fig. 9 is plotted in Fig. 10 alongside the DPEA pressure data as a function of strain. The legend depicts the average stress (or pressure) values of each curve as a percentage of their maximum values. In this way Fig. 10 demonstrates the pressure-volume curve flattening effect of the DPEA both qualitatively and quantitatively.

Even with an initial volume ratio $\forall_m/\forall_{f0}$ of only 6.1:1, the DPEA has an average-to-maximum pressure ratio that is 11 % higher than the average-to-maximum stress ratio of the material in uniaxial tension. Based on the initial volume ratio and maximum elongation, Eq. 4 predicts that this DPEA should have a fluid specific energy density equal to 43 % that of the material strain energy density.

Fig. 9: *Polyurethane of durometer 40A uniaxial tensile test with same specimen to be used in DPEA testing*

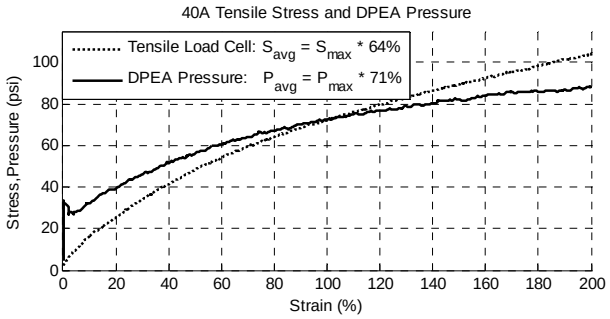

Fig. 10: *Comparison of DPEA charging prssure to uniaxial tensile stress as a function of elongation*

Applying Eq. 1 to the tensile data yields a strain energy density of 0.90 kJ/L (130 psi). Equation 2 tells us that the average pressure is equivalent to the fluid specific energy density, which is in this case 0.43 kJ/L (63 psi). The actual fluid specific energy density comes to 48 % of the material strain energy density, a close agreement with the theoretical prediction of 43 %.

7 Results and Conclusions

Construction of a full-scale prototype using the candidate 90A durometer polyurethane would require industrial grade tools. Preliminary attempts revealed the extreme challenge of creating low-profile grips capable of holding such a strong material at such high strains. As seen in Fig. 11, the best attempt to grip polyurethane 90A in a DPEA configuration resulted in grip failure at 350 psi at a mere 25 % elongation. This is a challenge that would need to be solved in order to commercialize the DPEA concept. There are a number of options for clamping that were not attempted due to cost and lack of necessary resources. Such options include casting the material around an insert, or casting it in clampable shapes, or bonding it to the piston and endcap, or combinations of these. Further work is needed in this regard and perhaps relevant work from the tire industry or such technology as pneumatic muscles could be drawn upon.

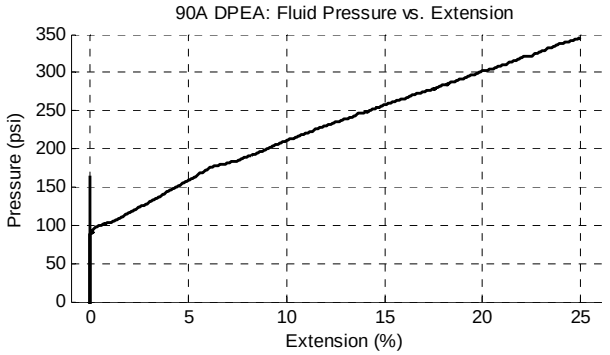

Fig. 11: *DPEA charging pressure prior to anchor slip*

In order to estimate the performance of such a device, however, the pressure/stress relationship observed in Fig. 10 was applied to tensile test data from Fig. 4.

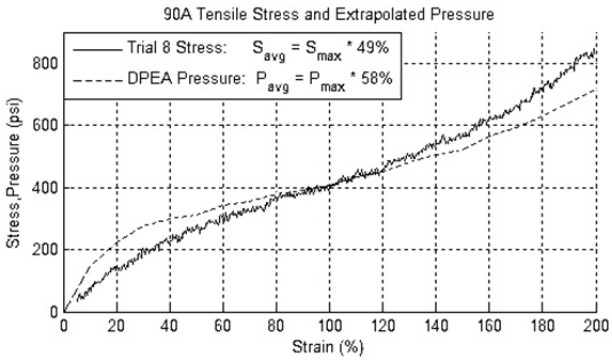

Fig. 12: *DPEA pressure/stress transmission ratios applied to 90A uniaxial tensile stress as a function of elongation*

The jagged line shows the tensile test data, while the smooth line is constructed from a sampling of the former line, scaled by the corresponding pressure/stress ratios observed in Fig. 10. Since the relationship between hydraulic pressure and material stress in a DPEA are geometric in nature, they should hold for any specimen of incompressible material, stressed from the same initial dimensions. Note that the pressure spike in Fig. 10 at 0 % strain has been omitted from the extrapolations in Fig. 12 because it is unclear if the spike is an artifact of static friction or a universal feature of DPEAs. Also note that the material strain has been limited to 200 % (rather than the optimal 300 % elongation) so that the ratios themselves would not have to be extrapolated. In this case, the average pressure and fluid specific energy density is 2.8 kJ/L (411 psi) while the strain energy density is 5.9 kJ/L (860 psi). According to Eq. 3 the total system energy density for a full scale DPEA using the candidate polyurethane stretched to 200 % elongation is therefore 1.9 kJ/L. This number is somewhat conservative, however, because the tensile data used for the extrapolation is an excerpt from Fig. 4 where the maximum elongation was 300 %. Mullins softening has therefore suppressed this segment of tensile data beyond that which it would normally experience from a peak elongation of 200 %.

Using Eq. 4 instead of Fig. 10 and 12, these energy densities can be predicted when the material is allowed to stretch to 300 %. In this case, the full strain energy density of 15.4 kJ/L is utilized, but more fluid is required as well. Equation 4 predicts a ratio $\frac{e_f}{e_M}$ of 29 % which corresponds to a fluid specific energy density of 4.4 kJ/L and a system energy density of 3.4 kJ/L. This value is about one third of the desired system energy density and would require a system volume of roughly 60 L (2.0 ft^3), not counting dead volume.

The primary contribution to this volume is the hydraulic fluid, taking up just over 45 L. However, a stiffer polyurethane, with a lower peak extension could greatly diminish this volume. Equation 4 shows that e_f/e_M is inversely proportional to ε_{max} in a DPEA. This relationship, confirmed by the DPEA prototype, gives direction for future improvement in DPEA design and construction. By evaluation candidate materials with Eq. 3 and 4 in mind, a material can now be chosen to maximize overall system energy density rather than strain energy density alone.

Utilizing the correct selection of $\varepsilon_{\max}$, it is useful to forecast the system energy density of the DPEA vs. conventional gas charged accumulators based on the experimental findings above and as a function of the strain energy density of other materials. This will extend the results to future selections of suitable materials. Ashby (Ashby, 1992) and modern material selection software (CES Selector, 2008) both indicate that elastomeric materials should extend upwards to 100 kJ/L in strain energy density.

By substituting Eq. 4 into Eq. 3, the DPEA accumulator has the following system energy density:

$$e_{\text{sys,DPEA}} = \frac{\mathrm{e_M}}{(\varepsilon_{\max}+1)\left(1+\frac{\forall_{\mathrm{f0}}}{\forall_{\mathrm{m}}}\right)} \tag{5}$$

where the maximum strain is given by:

$$\varepsilon_{\max} = \frac{\mathrm{e_M}}{\mathrm{e_f}\left(1+\frac{\forall_{\mathrm{f0}}}{\forall_{\mathrm{m}}}\right)} \tag{6}$$

To compare a feasible DPEA design to a gas-charged accumulator, consider the system energy density of a gas-charged accumulator under isothermal conditions between two states: state 1) pre-charged to P_1 with a dead volume of fluid of $\forall_{\mathrm{f0}}$, a gas volume of $\forall_1$ and a reservoir of volume $\forall_{\mathrm{f}}$ full of fluid, state 2) pressure of P_2 with a volume of fluid equal to $\forall_{\mathrm{f}} + \forall_{\mathrm{f0}}$, a gas volume of $\forall_2$ and a reservoir of volume $\forall_f$ empty of fluid. The system energy density, accounting for the reservoir volume and the dead volume is given as:

$$e_{\text{sys,gas charged}} = \frac{\mathrm{e_{gas}}}{1+\frac{\forall_{\mathrm{f0}}}{\forall_{\mathrm{m}}}+\left(1-\frac{\mathrm{P_1}}{\mathrm{P_2}}\right)} \tag{7}$$

where e_{gas} is the energy density of the gas found from the potential for an ideal gas to do work between pressures P_1 and P_2 under isothermal conditions:

$$e_{\text{gas}} = \mathrm{P_1 ln}\left(\frac{\mathrm{P_2}}{\mathrm{P_1}}\right) \tag{8}$$

Consider the comparison of five separate cases: two conventional gas charged accumulators, and three DPEA accumulators.

Table 2: Case study operational parameters

System	P_1 (MPa)	P_2 or $P_{\max}$ (MPa)	$P_{\text{ave}} = e_{\text{f}}$ (MPa)	$\forall_{\mathrm{f0}} / \forall_{\mathrm{n}}$
Gas 1	10.4	20.8	-	0.1
Gas 2	13.9	34.6	-	0.1
DPEA 1	-	34.6	20.1†	0.1
DPEA 2	-	59.7	34.6†	0.1
DPEA 3	-	119.0	69†	0.1

† Based on experimental projections from 90A material.

Using the equations above, the system energy density and maximum strain can be calculated:

These results are illustrated in Fig. 13 and 14. As expected, a higher material strain energy density gives rise to a higher system energy density. Given that the densities of the fluid and elastomeric materials are near 1 kg/L, the gravimetric energy density of these systems in kJ/kg are similar numerical values to their volumetric energy density (excludes the mass of the containment vessel). With regard to the containment vessel, recent progress on fully composite piston accumulators (Otte, et al. 2012) indicates a weight savings of 70 % to 80 % over typical steel piston accumulators. Such a technology made to house a DPEA accumulator with an appropriately high energy density elastomeric material offers the potential of a compact and lightweight energy density system.

Table 3: Case study energy densities and required strains

System	e_{gas} (kJ/L)	e_{M} (kJ/L)	e_{sys} (kJ/L)	$\varepsilon_{\max}$
Gas 1	7.19	-	4.5	-
Gas 2	12.67	-	7.5	-
DPEA 1	-	15 - 100	8.1 - 16.5	0.68–4.6
DPEA 2	-	15 - 100	9.8 - 25.1	0.39–2.7
DPEA 3	-	15 - 100	11.4 - 39.4	0.20–1.33

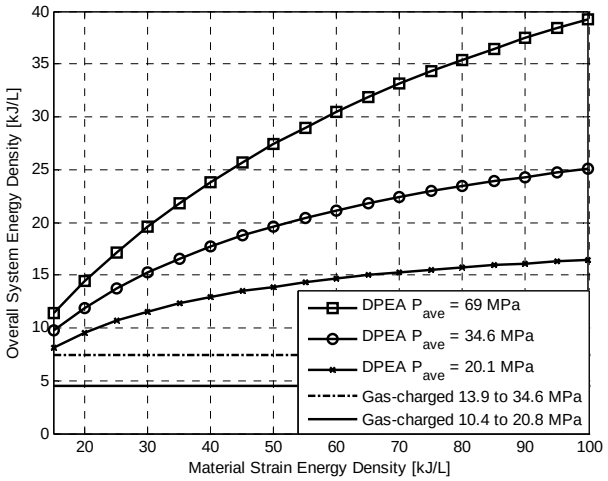

Fig. 13: *System energy density of DPEA as a function of material strain energy density operation at three different average pressures compared to two conventional gas-charged accumulators operating between 13.9 and 34.6 MPa (2000 to 5000 psig), and 10.4 and 20.8 MPa (1500 to 3000 psig)*

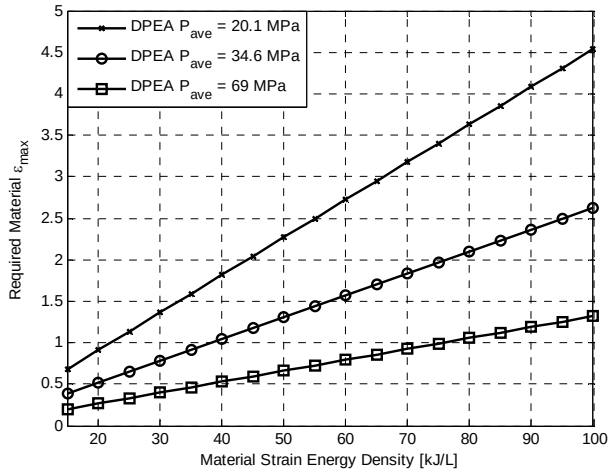

Fig. 14: *Required material elongation (maximum strain) of DPEA as a function of material strain energy density operating at three different average pressures*

Figure 14 is a useful conclusion in that as the operating pressure of the designed DPEA is increased, the required maximum elongation of the elastomer decreases. This illustrates the potential of this strain energy accumulator concept to overcome not only the gas diffusion difficulties of gas-charged accumulators, but to also not exceed material strain limits as the pressure increases; the DPEA concept is not limited by maximum elongation considerations.

The DPEA, like all strain energy accumulators, provides a solution to the gas diffusion problem which plagues conventional gas bladder accumulators. In addition, it maximizes material utilization while minimizing dead volume. The DPEA provides a predictable and favorable relationship between the stress-strain behavior of an elastomer and the fluid specific energy density of the accumulator which houses it. Consequently, the DPEA accumulator shows potential increases in volumetric system energy density over gas-charged accumulator systems.

Acknowledgement

This material is based upon work performed within the ERC for Compact and Efficient Fluid Power, supported by the National Science Foundation under Grant No. EEC-0540834.

Nomenclature

e_M	strain energy density	[kJ/L]
e_f	fluid specific energy density	[kJ/L]
$\forall_M$	material volume	[L]
$\forall_f$	working fluid volume	[L]
$\forall_{f0}$	initial (dead) fluid volume	[L]
ε_{max}	maximum elongation reached	[m/m]
σ_{max}	maximum stress reached	[MPa]

References

Ashby, M. F., Materials Selection in Mechanical Design, Pergamon, Oxford, 1992.

CES Selector ver. 4.8.0. Granta Design Limited. Build 2008, 2, 29, 1.

Diani, J., **Fayole, B.** and **Gilormini, P.** "A review on the Mullins effect" European Polymer Journal. Volume 45. Issue 3. March 2009 (pages 601 - 612)

Li, P., **Van De Ven, J. D.** and **Sancken, C.**, "Open Accumulator Concept for Compact Fluid Power Storage," Proceedings of the ASME International Mechanical Engineering Congress and Exposition, IMECE 2007, vol. 4, pp. 127-140, 2007.

Otte, B., **Stelling, O.** and **Müller, C.**, "High Pressure Lightweight Hydraulic Fully Composite Piston Accumulators" Proceedings of the 8th International Fluid Power Conference, Dresden, 2012.

Pedchenko, A. V. and **Barth, E. J.**, "Design and Validation of a High Energy Density Elastic Accumulator Using Polyurethane" Proceedings of the ASME Dynamic Systems and Control Conference 2009, DSCC2009, no. PART A, p 283-290, 2009.

Pourmovahed, A., **Baum, S. A.**, **Fronczak, F. J.** and **Beachley, N. H.**, 1988. "Experimental Evaluation of Hydraulic Accumulator Efficiency With and Without Elastomeric Foam". *Journal of Propulsion and Power*, 4(2), March-April, pp. 188.

Pourmovahed, A., 1988. "Energy Storage Capacity of Gas-Charged Hydraulic Accumulators". AIAA Thermophysics, Plasmadynamics and Lasers Conference, June 27-29, San Antonio, Texas. pp. 10.

Thapa, Khagendra, "Lithium Ion battery charging using bipolar transistors" Zetex Semiconductors http://www.diodes.com/_files/products_appnote_pdfs/zetex/an40.pdf, Issue 4, June 2007

Eric J. Barth
received the B. S. degree in engineering physics from the University of California at Berkeley, and the M. S. and Ph. D. degrees from the Georgia Institute of Technology in mechanical engineering in 1994, 1996, and 2000 respectively. He is currently an associate professor of mechanical engineering at Vanderbilt University, Nashville, TN and director of the Laboratory for the Design and Control of Energetic Systems. His research interests include the design, modeling and control of mechatronic and fluid power systems, energy storage, energy harvesting, power supply and actuation for autonomous robots, and MRI compatible robots.

John M. Tucker
received the B.S. and M.S. degrees in mechanical engineering from Vanderbilt University in 2010 and 2012 respectively. His research interests include mechanical design, mechatronic systems, and energy storage devices. He is currently employed as a technical support engineer for Laird Technologies, EMI Division, in Saint Louis, MO.